Available online at www.sciencedirect.com

ScienceDirect

Acta Materialia 55 (2007) 6453–6458

Acta MATERIALIA

www.elsevier.com/locate/actamat

Dissociated dislocations in confined plasticity

J. Douin *, F. Pettinari-Sturmel, A. Coujou

CEMES-CNRS, 28 Rue Jeanne Marvig, 31055 Toulouse cedex 4, France

Received 15 May 2007; received in revised form 2 August 2007; accepted 2 August 2007
Available online 20 September 2007

Abstract

The influence of the dissociation of dislocations when plasticity is localized in small volumes is illustrated for the case of γ/γ' superalloys. Dissociated dislocations constrained to move through channels present three different types of behavior. Dislocation dynamic simulations in a face-centered cubic crystal show these three types of behavior and give the conditions under which a dissociated dislocation can move through a channel bordered by impenetrable obstacles. We show that a partial dislocation needs a lower stress for its motion than a perfect one in a significant domain of stress orientations. The consequences of the uncorrelated motion of one of the partials, leading to the formation of large stacking faults, are also examined.

Keywords: Confined plasticity; Dislocations; Dissociation; Dislocation dynamics; Superalloys

1. Introduction

To strengthen a ductile crystalline material it is common practice to promote the formation of obstacles that partly inhibit the movement of dislocations, constricting their motion in small volumes. In Ni-based superalloys, this strengthening is essentially achieved by constraining the motion of dislocations within a soft face-centered cubic (fcc) γ matrix surrounded by hard $L1_2$ γ' precipitates. Recent developments [1] have shown that the best mechanical properties result from the presence of small tertiary γ' precipitates, which reduce the width of the channels for dislocation motion. This is a general behavior for particle-reinforced materials: the mean free interparticle distance strongly influences the yield stress (see e.g. Ref. [2] for particle-reinforced aluminum composites), and the smaller the interparticle distance, the larger the yield stress. In fact, the enhanced mechanical properties of most crystalline materials result from plasticity confined in small channels surrounded by strong or impenetrable obstacles.

When a dislocation is pushed towards the entrance of a channel between two obstacles, it must bend to enter the channel, and the increased strength of the material is ascribed to the stress needed for bending. The behavior of a dislocation under such confining conditions is difficult to model precisely for three main reasons: (i) the local properties of a dislocation change with the orientation of its line, and in particular its flexibility; (ii) each segment of the dislocation interacts with every other segment of dislocation, including itself; (iii) the dislocation strongly interacts with the local environment during its motion and its expansion is constrained to the shape of the channels.

Numerical analyses that take these effects into account have been used to study the behavior of dislocations geometrically confined in thin films [3–6], in epitaxial layers on a substrate [7], in metal/matrix composites [8] and in materials hardened by distributing small particles in the matrix [9–13]. However, an additional level of complexity results in the possible splitting of the dislocation into partial dislocations bounding a stacking fault (SF). Spontaneous splitting of a dislocation into partials is described in almost every textbook on dislocations (e.g. [14]) and simply result from a decrease in the total energy of the dislocation, which can be easily calculated provided the splitting width

* Corresponding author. Tel.: +33 5 62 25 78 73; fax +33 5 62 25 79 99.
E-mail address: joel.douin@cemes.fr (J. Douin).

1359-6454/$30.00
doi:10.1016/j.actamat.2007.08.006

is not too small [15]. Dissociation can also be initiated by a local event, in particular through locked dislocations undergoing a large stress [16]. This behavior can also result from the motion of a dislocation between obstacles, as observed by transmission electron microscopy (TEM) in NR3 [17,18] and MC2 [18] superalloys during situ experiments as well as in Astroloy [19] at a low strain rate. Such a dissociation process is illustrated in Fig. 1.

As the dislocations must bend to bypass the obstacles, the flexibility of the dislocations must be taken into account and the fact that partial dislocations have a larger flexibility than perfect ones may promote dissociation of the dislocations. The present paper intends to prove the importance of taking dissociation into account when deformation is limited to small volumes. We show that upon entering a channel surrounded by impenetrable obstacles, a perfect dislocation of a fcc crystal can be locked at the entrance of a channel while partial dislocations continue to propagate between obstacles. Furthermore, the trailing partial may also be unable to go through the channel, and we have studied the conditions of uncorrelated motion of partial dislocations resulting from the presence of the channel. We show that such a resulting dissociation and uncorrelated motion of one partial may have important implications for the mechanical behavior of such materials.

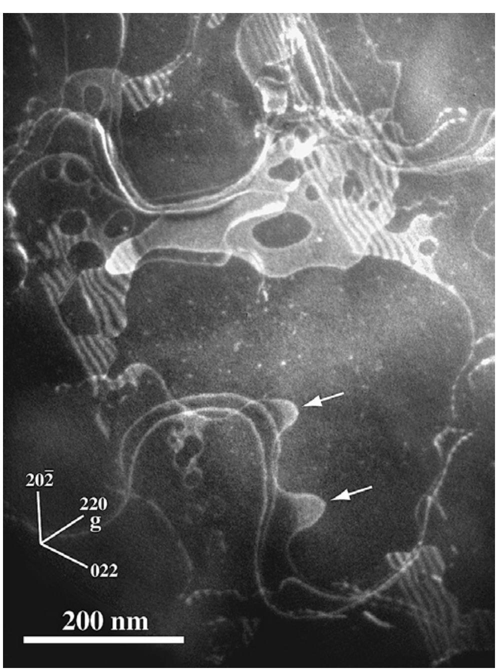

Fig. 1. Weak-beam micrograph of a MC2 superalloy deformed by creep. The foil is normal to the direction of the electron beam $[1\bar{1}1]$. In this material, the $a/2\langle 110\rangle$ dislocations propagate in small fcc γ-phase channels between $L1_2-\gamma'$ Ni_3Al precipitates (out of contrast here). Stacking faults are frequently observed. They present fringe contrasts for inclined $\{111\}$ fault planes and a constant grey contrast for the $(1\bar{1}1)$ fault plane parallel to the surface of the foil. A careful inspection shows that dissociation is initiated at the entrance of the channels (see arrows), leading to large stacking faults upon uncorrelated motion of the leading partial dislocation.

In particular, dissociation allows deformation for a stress much lower than the usual 0.2% strain elastic limit.

2. Analytical description

To enter a channel, a dislocation must bend (Fig. 2). The local curvature R of a dislocation is inversely proportional to the local force F acting perpendicularly to the segment according to $R = T/F$ [14], where the flexibility of the dislocation is accessed through its local character-dependent line tension T. To describe the effect of the changing curvature over the whole dislocation loop, we made use of the Wulff construction for dislocation problems [20,21]. The shape of a dislocation under a shear stress τ in the direction of its Burgers vector $\vec{b}$ is the inner envelope of the normals to the ends of the lines $E_s(\theta)/\tau b$, i.e. the pedal of the polar plot of $E_s(\theta)/\tau b$, where $E_s(\theta)$ is the self-energy per unit length of the dislocation with character θ. This analytical formulation neglects the long-range interaction between segments, but includes the variation of the line tension along the whole dislocation line. Owing to the mathematical properties of the pedal of a curve, the half-projected width of a dislocation loop in the direction θ of the channel is then given by $p(\theta) = E_s(\theta)/\tau b$ (Fig. 2). In this relation, τb is the force in the direction of $\vec{b}$ and in the glide plane. More generally, the force on the dislocation is related to the applied stress tensor $\bar{\bar{\sigma}}$ by the Peach–Koehler relation [22]. In what follows, and in order to explore all the directions of shear in the glide plane of the dislocation, we will call effective shear stress $\vec{\tau} = \bar{\bar{\sigma}}.\vec{n}$, where $\vec{n}$ is the unit vector normal to this plane. The modulus of the force acting perpendicular to a segment of dislocation in the plane defined by $\vec{n}$ is then $F = \vec{\tau}.\vec{b}$, and the modulus of the necessary stress to propagate by glide a dislocation through a channel of width H is then

$$\tau = \frac{2E_S(\theta)}{Hb\cos\varphi}. \tag{1}$$

Here φ is the angle between $\vec{\tau}$ and $\vec{b}$, and θ, the angle between the orientation of the channel and $\vec{b}$, can be viewed as the "channel character" (Fig. 2). It is worth emphasizing that Eq. (1), which represents isotropic and anisotropic elasticity, is consistent with the calculation proposed for a dislocation moving in a thin film [23].

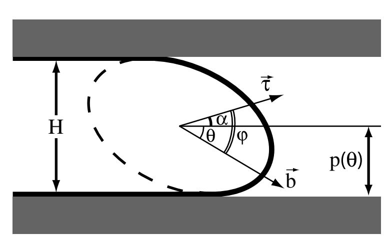

Fig. 2. Schematic shape of a dislocation gliding through a channel. The effective shear stress $\vec{\tau}$ is at angle α from the direction of the channel. The dashed line represents the shape of the complete loop whose projected size would fit the width channel H, under the effective shear stress $\vec{\tau}$.

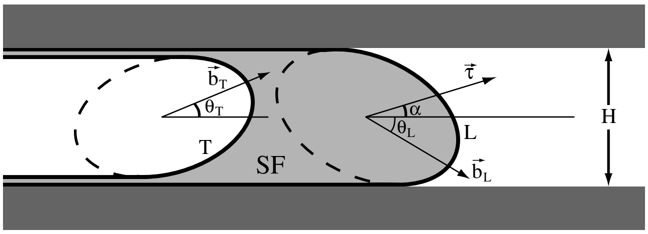

Fig. 3. Schematic shape of a dissociated dislocation gliding through a channel under an effective shear stress $\vec{\tau}$. The asymmetric shapes of the partials resulting from their different Burgers vectors were exemplified. Light grey area indicates the stacking fault (SF).

As the self-energy E_s of a dislocation is proportional to μb^2, the necessary stress to bend a dislocation decreases with the modulus of $\vec{b}$, and a partial dislocation should enter a channel more easily than a perfect one. The magnitude τ_L and τ_T of the effective shear stresses $\vec{\tau}$, at an angle α from the channel direction, required for the leading (L) and the trailing (T) partials bordering a stacking fault with energy γ to go through the channel differ by virtue of the fact that the fault opposes or helps the movement of the dislocations (Fig. 3).

Assuming isotropic elasticity, and neglecting self-interaction as well as interaction between partial dislocations, one finds

$$\tau_L(\alpha) = \left(\frac{2E_S(\theta_L)}{Hb_L} + \frac{\gamma}{b_L}\right)\frac{1}{\cos(\alpha+\theta_L)} \quad (2)$$

$$\tau_T(\alpha) = \left(\frac{2E_S(\theta_T)}{Hb_T} - \frac{\gamma}{b_T}\right)\frac{1}{\cos(\alpha-\theta_T)}. \quad (3)$$

Notice that as they have different Burgers vectors, the partials bend and propagate differently through the channel due to their different characters. Upon stress, the two Shockley partials may present asymmetric shapes (illustrated in Fig. 3), as observed by TEM [18,19] and retrieved by atomistic simulations in fcc-Al [24] or nanocrystalline Al [25]. Consequently, their separation distance changes in a complicated manner and there is thus no clear definition of the fault width.

3. Numerical simulations

Eqs. (1)–(3) neglect the interplay between dislocation flexibility, long-range interactions of dislocation segments, applied stress, and channel width and orientation. To take these properties into account, we have used a discrete dislocation dynamics simulation that includes all these different effects as well as dissociation, and aims to study the local effects as the interaction between dislocations and precipitates [26,27]. The dislocations are represented by a set of nodes connected by small segments rather than by straight segments of a given character chosen amongst a few numbers, usually screw and edge (see e.g. the extensive review in Ref. [28]). This allows a better description of the smallest changes in the orientation of the dislocations by alloying any character, and thus preserves even the smallest influence of the line tension. The simulation follows the now-classic scheme of calculating the force at a point in the dislocation from the total applied stress by using the Peach–Koehler formulation [22]. The motion of this point is obtained assuming a constant velocity proportional to the nodal driving force during a period of time. Without any lack of generality, calculations were made here for a dislocation dissociated into two Shockley partials in a fcc crystal according to the following reaction:

$$a/2[110] \rightarrow a/6[121] + SF + a/6[21\bar{1}] \quad (4)$$

in the $(1\bar{1}1)$ plane. $\vec{b}_L = a/6[121]$ and $\vec{b}_T = a/6[21\bar{1}]$ are the Burgers vectors of the leading and trailing partial, respectively, and we note $b = \|\vec{b}_L\| = \|\vec{b}_T\| = a/\sqrt{6}$.

The simulations were conducted for a dissociated dislocation moving in a channel surrounded by impenetrable obstacles, as is generally the case, for example, for channels between hard precipitates [17–19], between walls of dislocations [29] or within thin films [3,23]. Image forces have been taken into account with a good approximation by adding image dislocations parallel to the channel as described in Ref. [23] for dislocations moving in thin films. Including image forces, as well as geometrically necessary dislocations or misfit dislocations between precipitates and the matrix, would essentially result in an apparent narrowing of the channel, but would not change qualitatively the global behavior of the dislocations. For the sake of simplicity, these forces are not included here. In order to validate the approximations in our method, we have compared the result of the simulations with experimental observation: Fig. 4 shows the excellent agreement between the dislocation configuration generated by the simulation and the TEM observation of a dissociated $a/2[1\,1\,0]$ dislocation in the case of the fcc γ-phase of a Ni-based superalloy. The

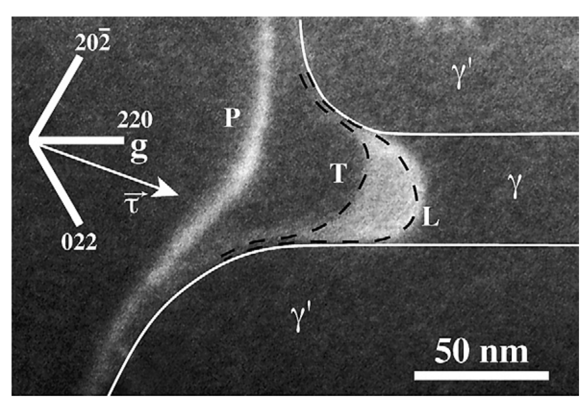

Fig. 4. Weak-beam micrograph of a $a/2[1\,1\,0]$ dislocation dissociated into two Shockley partial dislocations (L and T) trapped in a channel of a deformed MC2 superalloy. The γ' precipitates are out of contrast and are delimited by the white lines. The width of the channel is approximately 40 nm and the channel is oriented along the $[1\,1\,0]$ direction. The Burgers vectors of the L and T partial dislocations follow the reaction (4) and were determined using the $\vec{g} \cdot \vec{b} = 0$ criterion [32]. The shapes of the partial dislocations under the effective shear stress $\vec{\tau}$ with magnitude 450 MPa and at 20° from $[1\,1\,0]$ are superimposed on the figure (black dashed lines). The dislocation marked P is a perfect dislocation fully located in the γ-phase.

dislocation was moving in the $(1\bar{1}1)$ plane towards a 40 nm wide channel parallel to [1 1 0] and delimited by two impenetrable $L1_2$ precipitates. The elastic constants used are those of the γ-phase of a Ni-based superalloy [30]: the cell parameter are $a = 0.358$ nm, $\mu = 58.6$ GPa, $v = 1/3$ and the fault energy is $\gamma = 0.025$ J m^{-2} [31].

Fig. 5 summarizes the numerous dynamic simulations of dislocations performed assuming isotropic elasticity as in the fcc γ-phase of a Ni-based superalloy, as a function of stress magnitude and orientation and for a 50 nm wide channel. Examples of simulated configurations are also given in insets where the arrows represent the velocities of the partials. Fig. 5 shows that there are three possible types of behavior of a dissociated dislocation, as a function of the direction α and intensity τ of the effective shear stress: either none, only one, or both the partial dislocations go through the channel. The three areas respectively labeled 0, 1 and 2, separated by large dark curves, indicate the different types of behavior. For stresses in area 0, both partials are locked at the entrance of the channel. In area 1, the leading partial is moving through the channel while the trailing one is locked at the entrance, resulting in an irreversible separation of the two Shockley partials. For stresses in area 1* (separated from area 1 by line T), the leading partial is moving faster than the trailing one. Provided the channel is long enough, the width of the fault will attain a critical value of the order of several times the initial distance between partials, after which uncorrelated motion will also be effective. In areas 2, both partials go through the channel, either by decreasing (area 2) or increasing (area 2*) their separation distance from the equilibrium position under a symmetric effective stress parallel to [1 1 0].

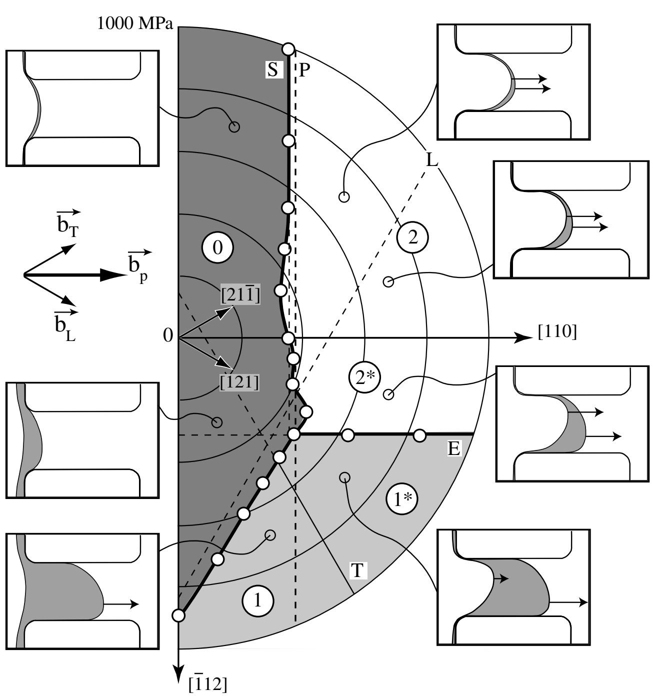

Fig. 5. Critical stresses for the different types of behavior of a [1 1 0] dissociated dislocation moving in the $(1\bar{1}1)$ plane of a MC2 alloy as a function of the effective shear stress $\vec{\tau}$ in the case of a 50 nm wide channel oriented in the [1 1 0] direction ($\theta_L = \theta_T = 30°$). Direction $[1\bar{1}1]$ is pointing downwards. The large dots indicating the limits for the different types of behavior are plotted in polar coordinates ($\|\vec{\tau}\|$, α), where $\|\vec{\tau}\|$ is in MPa and α is the angle of the direction of the stress $\vec{\tau}$ with the [1 1 0] direction. The numbers "0", "1" and "2" mark three areas and indicate the number of partial dislocations moving through the channel. Only stresses moving the whole configuration towards the channel are taken into account. The different lines correspond to the stress needed to overcome the channel in special cases: S, when correlated steady-state motion occurs; P, for an undissociated perfect dislocation; L, for the leading partial alone; T, for the trailing partial alone; and E, when uncorrelated motion occurs even in the absence of obstacles. The inserts show examples of simulations; arrows represent the velocities of the partials.

The dashed lines L and T in Fig. 5 respectively represent the limits defined by Eqs. (2) and (3). For stresses on the right-hand side of line L (respectively line T), a partial dislocation with $\vec{b}_L$ (respectively $\vec{b}_T$) Burgers vector trailing (respectively following) a stacking fault would be locked at the entrance of the channel. The horizontal line E corresponds to the limit $\tau = 2\gamma/(b\sin\alpha)$ for which, in the absence of obstacles, uncorrelated motion can occur due to the fact that the two partials are not moving at the same speed or in the same direction [24]. Thus, above line E, the motion of the two partial dislocations occurs in a correlated way. Notice that since $2\gamma/b$ is generally much higher than the critical resolved shear stress in materials with no confined plasticity, uncorrelated motion of partials is unlikely to appear, except if one manages to apply very high stresses [33]. When correlated steady-state motion occurs, the necessary stress to overcome the channel, defining the vertical line S, is

$$\tau_S(\alpha) = \frac{2E_S(\theta_d)}{Hb_P}\frac{1}{\cos\alpha}, \tag{5}$$

where $E_S(\theta_d)$ is the self-energy per unit length of the total dissociated dislocation with character θ_d and total Burgers vector $\vec{b}_P$. It is important to realize that if dissociation is energetically favorable, then τ_S is smaller than the stress τ_P necessary for the motion of an undissociated dislocation through the channel, since $\tau_P(\alpha) = \frac{2E_S(\theta_P)}{Hb_P}\frac{1}{\cos\alpha}$ with $E_S(\theta_P) > E_S\ (\theta_d)$ (line P parallel to S on Fig. 5).

From Fig. 5, it is clear that analytical approximations capture fairly well the behavior of the dislocations, even if they do not take interactions between segments into account (dashed lines in Fig. 5). It is obvious that for a much smaller channel width, the repulsive interaction between partials will be magnified, and thus the influence of long-range interaction intensified. However, we have checked that even for a very small 20 nm wide channel, the necessary stress for dislocation motion for $\alpha = 0°$ is 930 MPa, in good agreement with Eq. (5) which predicts 925 MPa. A decrease in the channel width would thus not modify qualitatively the conclusions drawn. This holds true for a change in the orientation of the channel: the simulation predicts a stress of about 500 MPa when the 50 nm wide channel is rotated by 60°, to be compared with the estimated value of 510 MPa given by Eq. (5).

4. Discussion

The important result in Fig. 5 is the existence of a range of stresses where the motion of a perfect dislocation through the channel is inhibited but plastic deformation is still made possible through the dissociation of the dislocation. This domain corresponds to the areas "*a*" and "*b*" (Fig. 6), which are parts of area 1 in Fig. 5, on the left-hand side of line *P* and separated by line *T*. For example, for an effective shear stress $\vec{\tau}$ parallel to [0 1 1] (Fig. 6), the magnitude of the stress needed to move the leading partial dislocation (point A) is about 30% smaller than that needed for the perfect dislocation (point B). Thus dissociation favors the motion of the dislocations and in this case a large stacking fault will be created, trailing an uncorrelated moving Shockley partial. This behavior arises for stresses oriented between about [1 3 2] and [$\bar{1}$ 1 2], i.e. for more than 25% of the stress orientations. In area "*a*", plastic deformation is provided by the uncorrelated motion of the leading partial dislocation, the trailing one being completely trapped at the entrance of the channel. When the stress orientation is close to [1 2 1], in area "*b*", both partial dislocations move through the channel, but with different velocities, the trailing one being slower due to the smaller force acting on it.

It is worth emphasizing that, for stresses oriented in the [$\bar{1}$ 1 2] direction, an undissociated dislocation would never move through the channel whatever the level of stress, while deformation is again made possible by the uncorrelated motion of a partial dislocation. Thus at a level of stress below what would be necessary for an undissociated dislocation to pass through (line P), dissociation provides a supplementary degree of freedom for dislocation motion. Predicting the mechanical properties requires that every key mechanism limiting or modifying the motion of dislocations be clearly pointed out and taken into account. When dislocation processes are intrinsic to the dislocation and occur independently of the geometry of the local microstructure, they are quite predictable, thus easily included in modeling. This is not the case when the behavior of the dislocations is controlled by their interactions with the nearby environment. The extent of area "*a*" indicates the necessity of including not only perfect dislocations but also partial dislocations bordering a stacking fault in any modeling of materials where channels between obstacles are significantly present.

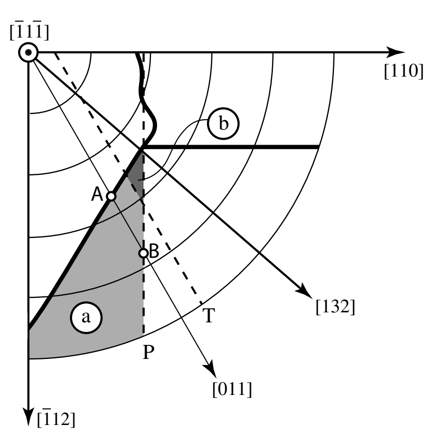

Fig. 6. Details of Fig. 5 showing the areas for which motion of one partial through the channel is possible while the stress is not sufficient to provide plastic deformation by means of a perfect dislocation motion. In area "*a*" the trailing partial is locked at the entrance of the channel and the leading partial moves through the channel, leading to full uncorrelated motion of the partial dislocations; in area "*b*", both partials move through the channel but with different velocities, also possibly resulting in an uncorrelated motion for a sufficiently long channel.

While allowing plastic deformation at a lower level of stress, such a process of completely moving apart partial dislocations has important implications for the future behavior of the materials. The activation of the uncorrelated motion of one partial dislocation induces changes in the future mobility of the whole dislocation, in particular by inhibiting the recombination of dislocations. As the parameters controlling the cross-slip probability are highly dependent of the probability of recombination of the two partials, the occurrence of cross-slip will drop to zero in the case of the uncorrelated motion of one partial. In the absence of recombination or a complexing mechanism—such as the Fleisher mechanism of cross-slip for which dislocation constriction is not required but a very high stress perpendicular to the fault plane is needed [34]—dislocation glide will be confined within the dissociation plane. It is worth recalling that in the early stages of deformation, both in monotonic and cyclic deformation, dislocation storage, and thus hardening, is directly related to the cross-slip mechanism [35]. It should also be pointed out that the activation of the uncorrelated motion of one partial will not be fully reversed upon removal of the applied stress. The intersection of the fault formed behind an uncorrelated partial by another $a/2\langle 1\,1\,0\rangle$ dislocation moving in a plane not parallel to the fault is accompanied by the formation of a jog on the $a/6\langle 1\,1\,2\rangle$ partials bordering the fault [16,36]. These jogs are generally sessile in the {1 1 1} plane of the fault and the energy required for the formation of the dislocation dipole, on the two edges of a jog, should be prohibitive. Stacking faults then act as barriers to the movement of dislocations and the deformation may become restrained in boxes surrounded by stacking faults [37].

It is finally important to emphasize here that the three types of behavior described above have been directly observed by TEM in different superalloys [17–19]. In what are probably the currently used materials with the best mechanical properties, such micromechanisms describe how the dislocations explore the microstructure, i.e. how deformation continues to occur through microplasticity in real-life conditions, e.g. creep, at a level of stress well below the stress needed to attain the 0.2% strain limit. This analysis, and particularly the influence of the larger flexibility of partial dislocations on their motion between obstacles, would extend to, and have consequences for, numerous other materials. In thin metal films on substrates, for example, passivated surfaces and/or interfaces with a substrate act as obstacles to dislocation glide and the very high strengths and high strain hardening rates are directly related to the effects of confinement on the motion of dislocations [23]. In these materials, it has been shown that deformation by partial dislocations becomes preferred as the film thickness decreases [38,39]. Several models have been proposed in which deformation twins are created by stacking faults led by preferentially nucleated $a/6\langle 1\,1\,2\rangle$ Shockley partial dislocations [38,40–42].

5. Conclusions

Through the demonstration of an efficient method to study the dynamic interactions between dislocations and obstacles, we have shown the remarkable influence of confined plasticity on the dissociation of dislocations. When plasticity is localized in small volumes, the dissociation of perfect dislocations favors their propagation. For about a quarter of the stress orientations, the uncorrelated motion of partial dislocations will be activated for a lower applied stress than the stress needed for the motion of a perfect dislocation. Dynamic simulations of dislocations also clearly show that the complex behavior of a dissociated dislocation moving towards a channel can be satisfactorily predicted by analytical predictions that neglect long-range interactions, as long as the channel width is not too small. This approach then provides an efficient method of determining the relevant parameters for large-scale calculations.

References

[1] Locq D, Caron P, Raujol S, Pettinari-Sturmel F, Coujou A, Clément N. In: Howson et al., editors. Proceedings of superalloys; 2004. p. 179.
[2] Kouzeli M, Mortensen A. Acta Mater 2002;50:39.
[3] Pant P, Schwarz KW, Baker SP. Acta Mater 2003;1:3243.
[4] von Blanckenhagen B, Arzt E, Gumbsch P. Acta Mater 2004;52:773.
[5] Ghoniem NM, Han X. Phil Mag 2005;85:2809.
[6] Mughrabi H, Pschenitza F. Phil Mag 2005;85:3029.
[7] Groh S, Devincre B, Kubin LP, Roos A, Feyel F, Chaboche J-L. Phil Mag Lett 2003;83:303.
[8] Groh S, Devincre B, Kubin LP, Roos A, Feyel F, Chaboche J-L. Mat Sci Eng 2005;400:279.
[9] Foreman AJE, Makin MJ. Phil Mag 1966:911.
[10] Zhu AW, Starke EA. Acta Mater 1999;47:3263.
[11] Mohles V, Nembach E. Acta Mater 2001;49:2405.
[12] Mohles V. Mat Sci Eng 2002;A324:190.
[13] Shin CS, Fivel MC, Verdier M, Oh KH. Phil Mag 2003;83:3691.
[14] Friedel J. Dislocations. Oxford: Pergamon Press; 1964.
[15] Saada G, Douin J. Phil Mag Lett 1991;64:807.
[16] Veyssière P, Douin J, Beauchamp P. Phil Mag A 1985;51:469.
[17] Décamps B, Raujol S, Coujou A, Pettinari-Sturmel F, Clément N, Locq D, et al. Phil Mag 2004;84:91.
[18] Raujol S, Benyoucef M, Locq D, Caron P, Pettinari F, Clément N, et al. Phil Mag 2006;86:1189.
[19] Saint-Antonin F, Ph.D thesis, 1991, Ecole des Mines de Paris.
[20] Burton WK, Cabrera N, Frank F. Phil Trans Roy Soc (London) 1950;A243:299.
[21] Hazzledine PM, Karnthaler HP, Korner A. Phys Stat Sol (a) 1984;81:473.
[22] Peach MO, Koehler JS. Phys Rev 1950;80:436.
[23] Nix WD. Scripta Met 1998;9:545.
[24] de Koenig M, Cai W, Bulatov VV. Phys Rev Lett 2003;91:25503.
[25] Van Swygenhoven H, Derlet PM, Frøseth AG. Acta Mater 2006;54:1975.
[26] Douin J, Donnadieu P, Epicier T, Dirras GF, Proult A, Silvain JF. Mat Sci Eng A 2002;319:270.
[27] Douin J, Donnadieu P, Finel A, Dirras GF, Silvain JF. Composites A 2002;33:1397.
[28] Ghoniem NM, Busso EP, Kioussis N, Huang H. Phil Mag A 2003;83:3473.
[29] Mughrabi H, Pschenitzka F. Phil Mag 2005;85:3029.
[30] Pollock TM, Argon AS. Acta Met 1994;42:1859.
[31] Pettinari F, Douin J, Saada G, Caron P, Coujou A, Clément N. Mat Sci Eng A 2002;325:511.
[32] Douin J, Veyssière P, Saada G. Phil Mag A 1998;77:1323.
[33] Rabier J, Demenet JL. Phys Stat Sol B 2000;222:63.
[34] Fleischer RL. Acta Met 1959;7:134.
[35] Kubin LP, Devincre B. In: Bilde Soerensen et al., editors. Deformation-induced microstructures: analysis and relation to properties. Roskilde: Riso National Laboratory; 1999. p. 61.
[36] Christian JW, Mahajan S. Prog Mat Sci 1995;39:1.
[37] Jouffrey B, Daniel A, Escaig B. J Phys C3 1966;27:114.
[38] Chen M, Ma E, Hemker KJ, Sheng H, Wang Y, Cheng X. Science 2003;300:1275.
[39] Oh SH, Legros M, Kiener D, Gruber P, Dehm G. Acta Met 2007;55:5558.
[40] Venables JA. Phil Mag 1961;6:379.
[41] Cohen JB, Weertman JR. Acta Met 1963;11:96.
[42] Lagerlöf KPD, Castaing J, Pirouz P, Heuer AH. Phil Mag A 2002;82:2841.